CONCRETE LIBRARY OF JSCE NO. 20, DECEMBER 1992

RATE PROCESS ANALYSIS OF ACOUSTIC EMISSION ACTIVITY IN CORE TEST OF CONCRETE

(Reprint from Proc. of JSCE, No. 442/V-16, pp. 211-217, February 1992)

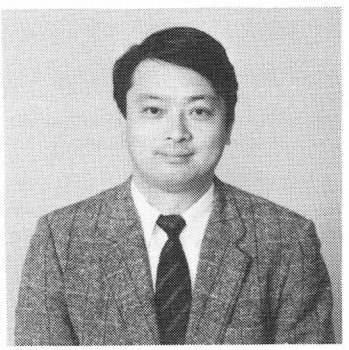

Masayasu OHTSU

SYNOPSIS

Acoustic emission (AE) activity under uniaxial compression is closely related with the existence of microcracks in concrete. When concrete contains a number of critical microcracks, AE events occur actively from the low stress level. In contrast, AE activity in sound concrete is observed just prior to final failure. The discrepancy of AE generating behavior is quantitatively evaluated, introducing the rate process theory. To gauge the applicability of AE rate process analysis to the uniaxial compression tests of core samples, experiments on newly cast concrete and core samples are carried out. The core samples of controlled damage were taken from reinforced concrete slabs which were tested by cyclic fatigue loading. Thus, the correlation with the strength, the age, and the damage level of concrete is clarified.

Keywords: acoustic emission, concrete core, uniaxial compression test, rate process analysis

---

M. Ohtsu is a professor in the Department of Civil and Environmental Engineering at Kumamoto University, Kumamoto 860, Japan. He received the degrees of B. S. in 1974, M. S. in 1976, and Dr. Eng. in 1983 from the Department of Civil Engineering at Kyoto University. He is involved in international work on applications of acoustic emission to concrete and nondestructive evaluation of concrete structures. He serves as an active member of technical committees in JSCE, JCI, JSNDI and is also an associate member of the ACI committee 228 on nondestructive testing.

---

1. INTRODUCTION

Recent AE research in concrete engineering is roughly classified into two fields. One is associated with fracture mechanics [1], and the other is nondestructive evaluation (NDE) of structures [2],[3]. Because a large number of concrete structures, in particular those built in the 1960s, are found to be approaching their service limit due to severe environmental conditions and malfunction of materials, the development of diagnostic NDE is urgently required. AE applications to NDE in concrete structures are promising, but are not yet considered to be practical.

To develop a practical use of the AE technique, application to a uniaxial compression test of a core sample is investigated. Core samples are drilled from concrete structures and are usually tested to measure uniaxial compressive strengths and elastic moduli. In addition to these mechanical properties, measurement of AE activity under loading is proposed. Generating behavior of AE events is quantitatively analyzed, based on the rate process theory [4]. To gauge the applicability of the proposed procedure, newly cast concrete samples and core samples of controlled damage are tested. The relation between AE activity in the uniaxial compression test of core samples and concrete properties is clarified.

2. RATE PROCESS ANALYSIS

The Kaiser effect is well known as an irreversible AE generating behavior under uniaxial compression. It results from the fact that cracks nucleated due to previous loading do not propagate until the load exceeds the former level in the next loading. However, limited success is reported in respect to the determination of the previous load level, because it depends highly on the loading path and history. In usual cases, AE activity under uniaxial compression is observed from a low stress level. This is because the loading path is not identical to the previous path. This leads to the conclusion that some critical microcracks in a loading path normally propagate due to stress applied. When concrete contains a number of critical microcracks, active AE generation is expected from a low stress level due to new crack propagation. In contrast, AE activity in concrete of few microcracks is considered to be stable and low at a low stress level. Thus, the number of critical microcracks in concrete could be evaluated by monitoring AE activity under uniaxial compressive stress. This has already been confirmed by core tests of an old bridge [5].

To quantify the AE activity in the uniaxial compression test, the rate process theory is introduced. The probability function f(V) of AE occurrence from stress level V (%) to V+dV (%) is assumed as follows:

$$f(V)dV = dN/N, \tag{1}$$

where N is accumulated AE events up to stress level V (%), which is normalized by the failure load. Here, we assume the probability function f(V) as the following hyperbolic function,

$$f(V) = a/V + b, \tag{2}$$

where a and b are empirical constants. In the conventional rate process theory, the probability function f(v) is usually assumed as constant, which is called a rate, whereas Eq. 2 suggests two possible relations between the probability of AE occurrence and stress, introducing the hyperbolic term, a/V. The relation is illustrated in Fig. 1. In the case that the value 'a' is positive, the probability of AE occurrence is high at low stress level. In contrast, the probability is very low at low stress level when the value 'a' is negative. Since the discrepancy of 'a' values is considered to be dependent upon the amount of critical microcracks, the deterioration due to microcracking could be quantitatively evaluated on the basis of the value 'a'. From Eqs. 1 and 2, the

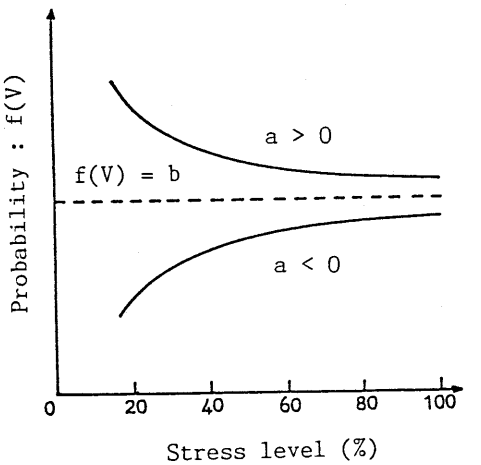

Fig. 1 Hyperbolic probability functions f(V) to analyze AE generating behaviors based on the rate process theory.

relationship between the number of total (accumulated) AE events N and stress level V (%) is obtained,

$$N = C\, V^{a} \exp(bV), \tag{3}$$

where C is an integration constant.

Equation 3 represents the relation between AE events and stress level. In the analysis, experimental data on AE events versus stress are approximated by Eq. 3, and three constants, a, b, and C, are determined by the least square error analysis.

3. TEST PROCEDURE

3.1 Specimens

All mix proportions of concrete tested are indicated in Table 1. For newly cast concrete, specimens of air-entrained concrete and steel-fiber reinforced concrete were made. Ordinary Portland cement was employed and the maximum gravel size was 20 mm. For air-entrained concrete, air contents were controlled at 3%, 5%, 7%, and 8% of concrete volume, by using air-entraining admixture. These are labeled AEC3, AEC5, AEC7, and AEC8, respectively. For steel-fiber reinforced concrete, shear-cut steel fibers of dimensions 0.5 mm x 0.5 mm x 30 mm were mixed at 1%, 2%, and 3% of concrete volume. These are labeled SFR1, SFR2, and SFR3 in Table 1.

For uniaxial compression tests, cylindrical specimens of 10-cm diameter and 20-cm height were cast. After moisture curing for 28 days, the three AEC3, AEC5, and AEC7 specimens were tested to determine the relationship between 'a' values and strengths. For AEC8 specimens, the effect of age was investigated. Twelve specimens were cast and three of them were tested at the age of one, two, three, and four weeks of moisture curing.

For core samples, early-strength Portland cement was employed and the maximum gravel size was 25 mm. The mix proportion is indicated as CORE in Table 1. Although the mix proportion looks the same as AEC8, the gravel size and the amount of admixture are different. As a result, the air content measured is slightly different from AEC8.

Table 1 Mix proportions of concrete

Specimen	Water	Cement	Sand	Gravel	Air	Fiber
	(kg per 1 m^3 of concrete)				(%)	(%)
AEC3	175	337	740	1181	3	-
AEC5	175	337	718	1147	5	-
AEC7	175	337	697	1113	7	-
AEC8	161	298	798	1052	8	-
SFR1	175	337	707	1130	5	1
SFR2	175	337	697	1112	5	2
SFR3	175	337	686	1095	5	3
CORE	161	298	798	1052	6	-

Table 2 Summary of RC slabs tested

Specimen	Load level:S (x Ps)	Crack density (m/m^2) Rank	Measured	Number of fatigue cycles
TP-1	Ps=42.5t	-	-	-
TP-2	0.4	A_0	12.0	10^4
TP-3	0.3	(10-12)	8.1	$5x10^4$
TP-4	0.3		10.7	$8x10^5$
TP-5	0.2	A	6.7	$2x10^6$
TP-6	0.3		8.1	$2x10^3$
TP-7	0.3	(7-8)	9.9	$3x10^3$
TP-8	0.25		8.5	10^2
TP-9	0.25		8.6	$3.5x10^4$
TP-10	0.19	C (3-4)	3.5	$7x10^3$

Ten reinforced concrete (RC) slab specimens of dimension 400 cm x 260 cm x 16 cm were cast. Fatigue experiments due to flexural loading on these specimens were reported in the previous paper [6]. RC slabs are named TP–1 to TP–10. All specimens were simply supported along the major edges and kept free along the traverse edges. In the TP–1 specimen, the loading plate was located at the center and loaded monotonously up to the final failure. Its failure load, Ps, was 416.5 kN (42.5 tons).

According to extensive studies on the deterioration of RC slabs in highway bridges, it is known that crack patterns generated in in–service RC slabs are quite different from those observed in one–point cyclic loading experiments [7]. The main discrepancy results from the moving effect of traffic vehicles. To take into account this effect, cyclic loading repeated at three locations was carried out at the load levels prescribed, such as 40 % of static bearing capacity (416.5 kN) for the TP–2 specimen and 30 % for TP–3. These are summarized as the load level, S, in Table 2. The degree of Deterioration of RC slabs is indicated by the crack density, which is obtained as the averaged total crack length per unit square meter panel. The RC slab specimens of controlled damage are classified into three ranks, such as Rank Ao, 10 to 12 m/m^2, Rank A, 7 to 8 m/m^2, and Rank C, 3 to 4 m/m^2. Crack propagation was traced during each test and the final crack density was measured at the central region of dimensions 100 cm x 100 cm. Since it is known that the crack density varies depending on many factors of measuring conditions, classification of the degree of deterioration was made, referring to the S–N curves [7]. Thus, the TP–3 specimen was classified into Rank Ao, whereas the crack density could belong to Rank A. After the tests of RC slabs, core samples of 10–cm diameter were drilled in each RC slab.

An example of core–drilled locations is shown in Fig. 2. Core–drilled locations of TP–2, TP–4, TP–5, and TP–6 specimens are shown. These locations are selected in order to prevent surface cracks from running across core samples. According to the previous results [8], mechanical properties of core samples taken from RC slabs cyclically loaded are not so dependent upon the core–drilled location as in the case of one–point static loading. After being taken from the RC slabs, the top and the bottom surfaces of core samples were ground in parallel, and thereby heights of the samples became approximately 15 cm.

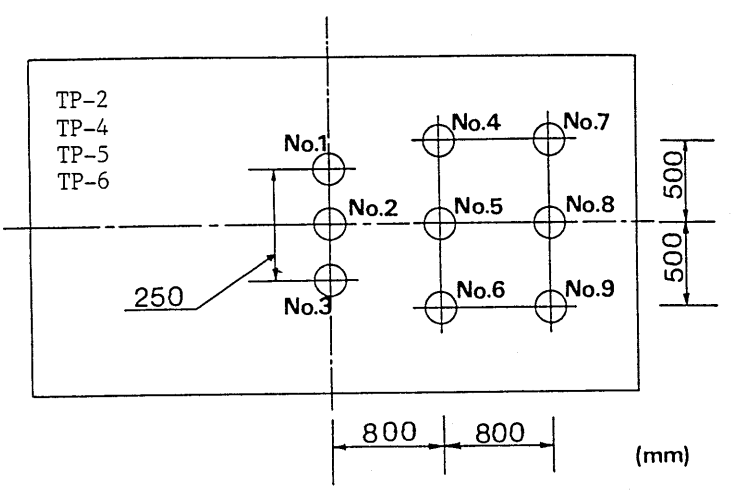

Fig. 2 Core–drilled locations in RC slabs.

3.2 Experiments

In a uniaxial compression test, AE events were counted up to the final failure by event counting. An AE sensor of 1 MHz resonant frequency was attached at half height of a cylindrical specimen. To decrease noise from contact surfaces between the specimen and loading plates, teflon sheets of 0.5 mm thickness with silicone grease were inserted. Total gain of AE measurement was set at 60 dB and the frequency range employed was 10 kHz to 300 kHz.

4. RESULTS OF RATE PROCESS ANALYSIS

4.1 Newly cast samples

AE observation in one of the AEC5 samples is shown in Fig. 3. A hatched histogram shows the relation between total AE event counts and stress level in a uniaxial compression test. The relation is approximated by Eq. 3, and constants a, b, C are determined as seen in the graph. The result of the approximation is indicated by a cross-hatched histogram. Note that the number of accumulated AE events is plotted at each 20 % increment of stress level in Fig. 3. Therefore, an overdetermined system of five relations between the number of AE, N, and the stress level V, is obtained to determine the three constants, by substituting into Eq. 3. In the graph, r means a correlation coefficient between the experimental data (hatched histogram) and the approximated data (cross-hatched histogram). A very close correlation, r = 0.997, is obtained. It implies that AE activity in the uniaxial compression test is reasonably approximated by Eq. 3. As can be seen, the value 'a' determined is negative, because the specimen is newly cast.

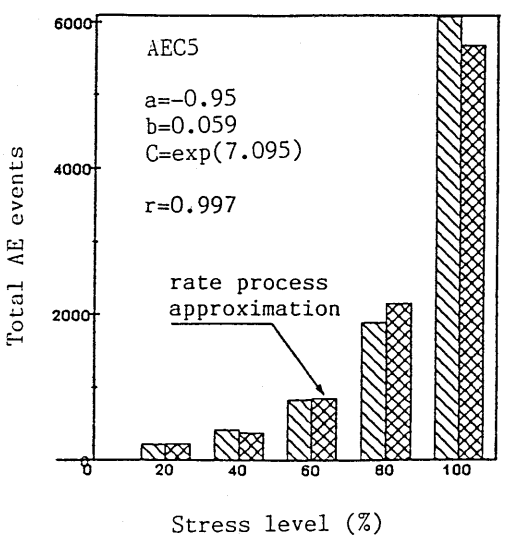

Fig. 3 AE activity versus stress level during a uniaxial compression test of AEC5 sample.

In newly cast samples of AEC3, AEC5, AEC7, SFR1, SFR2, and SFR3, the relation between the compressive strength and the value 'a' was investigated. Both the compressive strength and the value 'a' were determined from the average of three specimens. Results are shown in Fig. 4. A strong correlation between negative 'a' values and compressive strengths is found. It implies that concrete samples of high strength generate few AE events at low stress level. In other words, AE events begin to be generated at a higher stress level with the increase of the compressive strength.

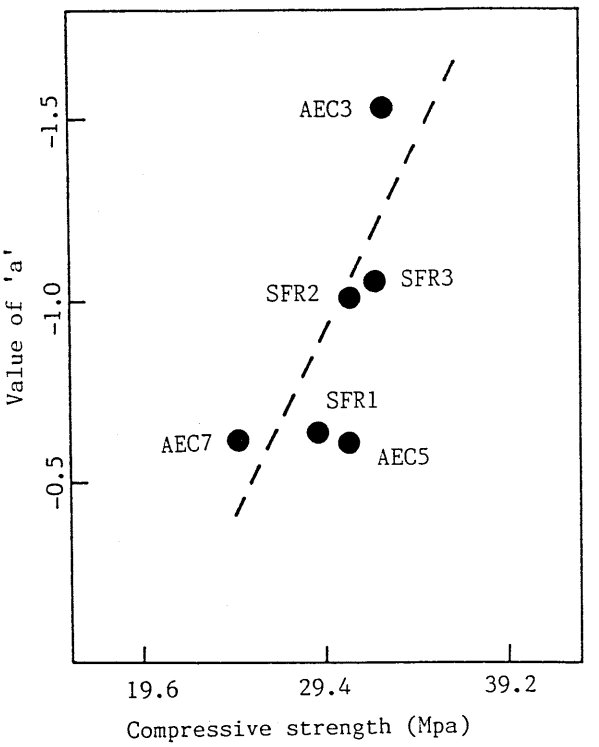

Fig. 4 Relations between compressive strengths and 'a' values in newly cast concrete samples.

In AEC8 specimens, uniaxial compression tests were performed at one, two, three, and four weeks elapsed. Results are shown in Fig. 5. Because the strength increases with the curing age, 'a' values become more negative with increasing age. These results agree well with those of Fig. 4.

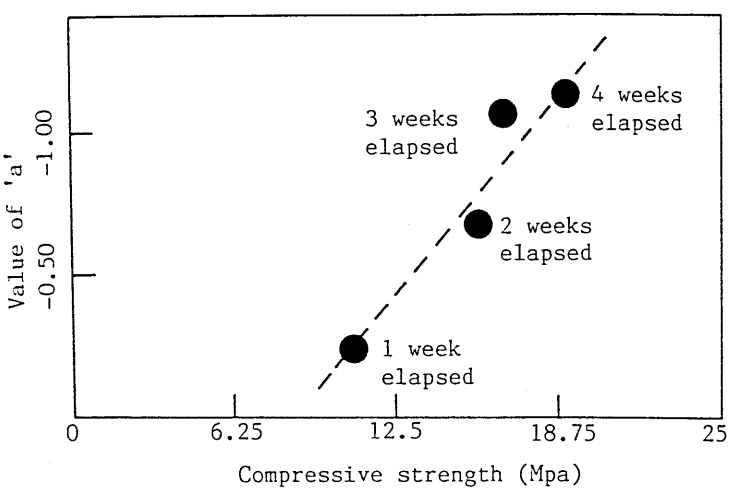

Fig. 5 Relations between compressive strengths and 'a' values at the ages of one week, two weeks, three weeks, and four weeks elapsed.

4.2 Core samples

All core samples extracted were tested under uniaxial compressive stress. Examples of results are shown in Fig. 6. It is observed that essential features of AE behaviors in both samples are remarkably recovered by the rate process approximation. The value of 'a' is negative in the No. 2 core sample of the TP–4 specimen, while it is positive in the No. 2 sample of the TP–5 specimen. Since the TP–5 specimen was loaded up to the maximum number of cycles, this result suggests that the concrete of the TP–5 specimen is heavily damaged. Although the TP–4 specimen shows high crack density (Rank Ao), the 'a' value of the core is negative. This may suggest that concrete of high crack density does not necessarily contain many microcracks.

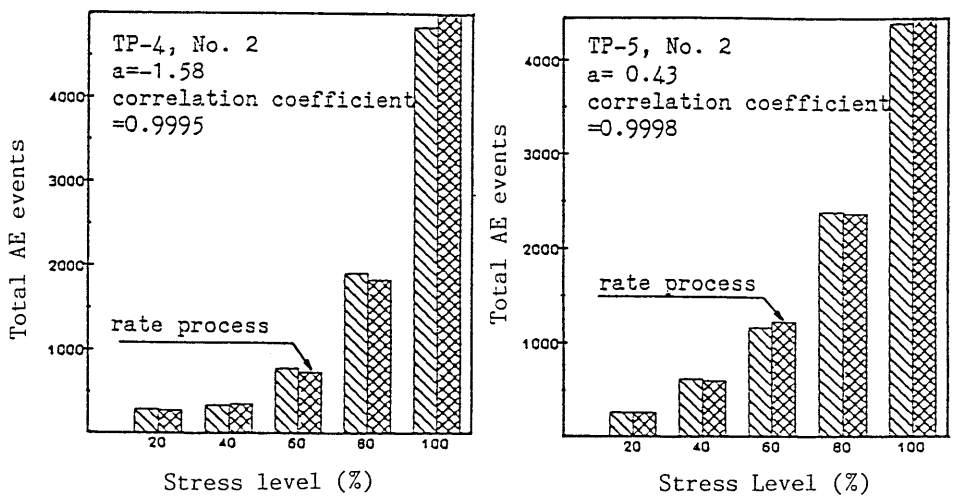

Fig. 6 Total AE events versus stress level in core samples.

To confirm the existence of microcracks in concrete, ultrasonic inspection of core samples was carried out. As shown in Fig. 7, ultrasonic waves of sweep mode were driven into core samples and frequency responses of cores were measured. This procedure is already proposed as a technique to obtain spectral responses in ultrasonic testing [9].

Ultrasonic waves propagate in a concrete member, and then scattering of waves is observed. Scattering, in principle, results from the fact that ultrasonic waves of shorter wavelength than the size of an obstacle cannot pass through the obstacle. The velocity of the P wave in concrete is approximately 4000 m/s. Consequently, frequency components of over 100 kHz (0.01 ms period) correspond to wavelengths of less than 40 mm. Provided that a core sample contains a number of microcracks of less than 40 mm in length, frequency components of over 100 kHz are not observed in the spectra. In Fig. 8, frequency spectra obtained in core samples taken from TP–5 and TP–10 specimens are shown. Frequency components of over 100 kHz are not observed in the core of the TP–5 specimen, while some responses in the frequency range from 100 kHz to 300 kHz are observed in that of the TP–10 specimen. According to Table 2, the TP–10 specimen is the least deteriorated. The bottom graph in Fig. 8 confirms this fact, while the top graph shows that core samples of the TP–5 specimen contain a number of microcracks of less than 40 mm. After the spectral responses of these cores were obtained, uniaxial compression tests were performed. The 'a' values determined from the rate process analysis are also shown in the figure. For the core of the TP–10 specimen, a = –1.61, while a = 0.05 in the core of the TP–5 specimen. These values confirm that the amount of microcracks in concrete can be evaluated quantitatively by rate process analysis.

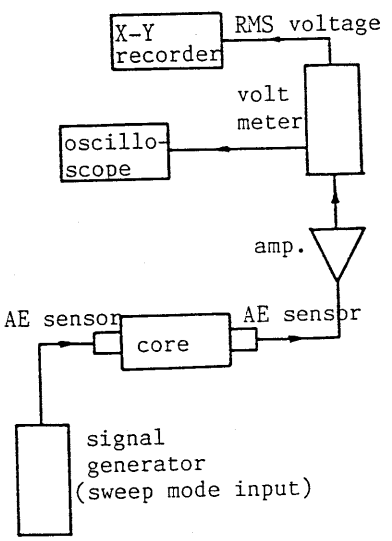

Fig. 7 Experimental setup for measuring spectral responses of cores.

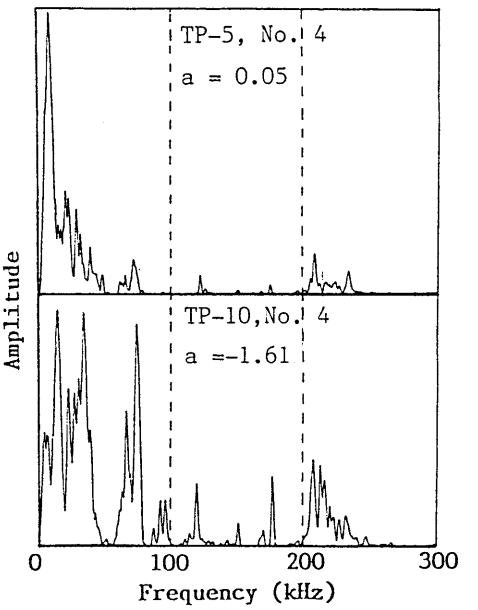

Fig. 8 Frequency spectra in core samples.

As shown in Table 2, the TP–5 specimen was loaded up to the maximum number of cycles. As a result, the 'a' values of core samples were all positive, although the crack density measured is the lowest except for TP–10. The maximum crack density is observed in the TP–2 specimen, whereas the 'a' values of core samples are negative. Since the crack density was measured only in the central portion, the averaged 'a' value of cores taken from centerline locations of the slab (for example, core No. 1 to No. 3 in Fig. 2) was determined. Results are summarized in Fig. 9. In accordance with the rank of the crack density in Table 2, plotted data are classified into three groups. Because positive 'a' values correspond to the existing large amount of microcracks, results imply that concrete cores of rank A contain the most potentially critical microcracks. In contrast, cores of rank Ao are shown to contain a small number of microcracks.

The crack density is associated with visible cracks and its value is known to be saturated at nearly 12 m/m^2 [7]. Consequently, results suggest that critical microcracks have already developed into visible cracks in RC slabs of rank Ao, and thus the concrete core of the noncrack region has a few microcracks. This implies that the amount of potentially critical microcracks may not be measured by visual inspection, but could be evaluated by the rate process analysis of AE activity in the core tests.

In actual bridge slabs, cracks are generated due to heavy traffic loads. Under repeated loading, microcracks in the noncracked region are accumulated and coalesced as visible cracks, which can contribute to the growth of the crack density. In the saturated stage of the crack density, however, crack motions are localized in the existing cracked region and new cracks are not observed. This implies that potentially critical microcracks, which are responsible for the increase of the crack density, have exhaustively grown as visible cracks and the noncracked region at the final stage contains few microcracks. This may be one reason why core samples taken from the noncracked region in Rank Ao exhibit soundness. It is concluded that the amount of potentially critical microcracks in RC slabs may be evaluated at the stage of Rank A by the rate process analysis of AE activity in the core sample under uniaxial compression.

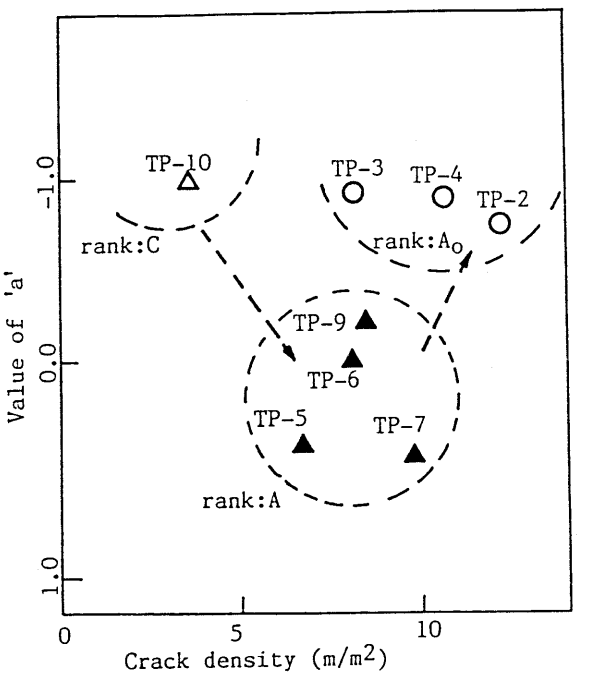

Fig. 9 Relations between crack densities of RC slabs and 'a' values in core tests.

5. CONCLUSIONS

To assess the deterioration of concrete structures, a method to analyze AE activity of core samples under uniaxial compression is proposed. To quantify AE generating behaviors, the rate process analysis is introduced, by assuming a hyperbolic function of the probability on AE generation. The applicability of the procedure is studied in newly cast samples and core samples of controlled damage. The core samples were taken from the RC slabs tested by cyclic loading.

Results obtained are summarized as follows:

(1) The effects of the strength and the age of concrete on the 'a' values in the AE occurrence probability are obtained. This demonstrates that high-strength concrete generates few AE events at a low stress level.

(2) The relation between microcracks contained in concrete and the 'a' values is confirmed by ultrasonic spectroscopy. The process of deterioration in RC slabs is elucidated from the rate process analysis of AE activity in core tests.

Although an extensive study is still needed to link the value of "a" with the deterioration degree of concrete, the empirical relation between the value of "a" and the crack density in the RC slab is found. The results confirm that the rate process analysis of AE activity provides information on the amount of potentially critical microcracks in concrete.

ACKNOWLEDGEMENTS

The author wishes to thank Drs. S. Yuji and Y. Kawai of Kawasaki Steel Corporation for their support in the experiments on RC slabs. Cyclic experiments on the RC slabs were carried out by utilizing their facility. The author also thanks Prof. T. Sakimoto, and Messrs. H. Morinaga and K. Masuda of Kumamoto University for their valuable assistance in this research.

REFERENCES

[1] Maji, A. K. and Shah, S. P.,"Application of Acoustic Emission and Laser Holography to Study Microfracture in Concrete," Nondestructive Testing, ed. H. S. Lew, ACI SP-112, 83-109, 1988.
[2] Ohtsu, M.,"Acoustic Emission Characteristics in Concrete and Diagnostic Applications," Journal of Acoustic Emission, Vol. 6, No. 2, 99-108, 1987.
[3] Uomoto, T.,"Application of Acoustic Emission to the Field of Concrete Engineering," Journal of Acoustic Emission, Vol. 6, No. 3, 137-144, 1987.
[4] Ohtsu, M., Sakimoto, T., Kawai, Y. and Yuji, S.,"Evaluation of Concrete Structure Deterioration via AE Observation of Core Tests," Journal of Acoustic Emission, Vol. 7, No. 4, 167-172, 1988.
[5] Ohtsu, M.,"Diagnostics of Cracks in Concrete Based on Acoustic Emission," Nondestructive Testing, ed. H. S. Lew, ASTM, SP-112, 63-82, 1988.
[6] Yuji, S., Kawai, Y., Ohtsu, M. and Sakimoto, T.,"A Diagnostic Approach for RC-Slabs Based on Traveling Repeated Loading Tests," Journal of Structures and Materials in Civil Engineering, KABSE, No. 4, 61-68, 1989.
[7] Matsui, S.,"Fatigue Strength of RC-Slabs of Highway Bridges by Wheel Running Machine and Influence of Water on Fatigue," Proc. of the Japan Concrete Institute, Vol. 9, No. 2, 627-632, 1987.
[8] Ohtsu, M., Kawai, Y., and Yuji, S.,"Evaluation of Deterioration in Concrete by Acoustic Emission Activity," Proc. of the Japan Concrete Institute, Vol. 10, No. 2, 849-854, 1988.
[9] Sakata, Y. and Ohtsu, M.,"Crack Evaluation in Concrete by Ultrasonic Spectroscopy," Proc. Japan Society of Civil Engineers, No. 414/V-12, 69-78, 1990.